Thin-Walled Structures 90 (2015) 95–106

Contents lists available at ScienceDirect

Thin-Walled Structures

journal homepage: www.elsevier.com/locate/tws

Parametric and non-parametric probabilistic approaches in the mechanics of thin-walled composite curved beams

M.T. Piovan [a,*], R. Sampaio [b]

[a] Centro de Investigaciones de Mecánica Teórica y Aplicada, Universidad Tecnológica Nacional FRBB, 11 de Abril 461, B8000LMI Bahía Blanca, Argentina
[b] PUC-Rio, Mechanical Engineering Department, Rua Marquês de São Vicente 225, 22451-900 Rio de Janeiro, RJ, Brazil

ARTICLE INFO

Article history:
Received 8 September 2014
Received in revised form
20 December 2014
Accepted 21 December 2014

Keywords:
Uncertainties quantification
Composite curved beams
Dynamics
Flexible structures

ABSTRACT

In this paper we perform a quantification of the uncertainty propagation of the dynamics of slender initially curved structures constructed with fiber reinforced composite materials. Depending on the manufacturing process, composite materials may have deviations with respect to the expected response, often called nominal response in a deterministic sense. The manufacturing aspects lead to uncertainty in the structural response associated with constituent proportions, material and/or geometric parameters among others. Another aspect of uncertainty that can be sensitive in composite structures is the mathematical model that represents the mechanics of the structural member, that is: the assumptions and type of hypotheses invoked reflect the most relevant aspects of the physics of a structure, however in some circumstances these hypotheses are not enough, and cannot represent properly the mechanics of the structure. Uncertainties should be considered in a structural system in order to improve the predictability of a given modeling scheme. There are two approaches to evaluate the propagation of uncertainties in structural models: the parametric probabilistic approach and the non-parametric probabilistic approach. In the parametric, one quantifies the uncertainty of given parameters (such as variation of the angles of fiber reinforcement and material constituents) by associating random variables to them. In the non-parametric, the propagation of uncertainty is quantified by considering uncertain the matrices of the whole system. In this study a shear deformable model of composite curved thin-walled beams is employed as the mean or expected model. The probabilistic model is constructed by adopting random variables for the uncertain entities (parameters or matrices) of the model. The probability density functions of the random entities are derived appealing to the maximum entropy principle under given constraints. Once the probabilistic model is discretized in the context of the finite element method, the Monte Carlo method is employed to perform the simulations. Then the statistics of the simulations is evaluated and the parametric and non-parametric approaches are compared.

1. Introduction

Composite materials have such a number of interesting features that impel their use in different industrial devices. Examples of these features are high strength and stiffness properties together with a low weight, good corrosion resistance, enhanced fatigue life, low thermal expansion properties among others [1]. The very low machining cost for complex structures is the other important feature of composite materials [2]. Slender composite structures that can be analyzed by means of curved beam models are present in many applications such as bridge segments, machine parts: such as leaf springs of sport cars or blades of turbo-propellers, among others.

The development of theoretical and computational methods for dynamic and static analysis of slender thin-walled composite structures is growing continuously since the early eighties. Thus, one of the first consistent studies about thin-walled composite-beams was introduced by Baud and Tzeng [3], who developed a beam theory to analyze fiber-reinforced members featuring open cross-sections with symmetric laminates invoking Vlasov's hypotheses. Afterwards, Bauchau [4] incorporated some aspects of shear flexibility in the analysis of thin-walled composite beams. Models of fiber reinforced composite beams that are based on Vlasov or Bauld and Tzeng's ideas [3] normally over-predict the values of natural frequencies and consequently the dynamic patterns, specially in the case of shorter beams. In the 1990s, many new models of composite beams were introduced, in which

* Corresponding author.
E-mail addresses: mpiovan@frbb.utn.edu.ar, mtpforever@gmail.com (M.T. Piovan), rsampaio@puc-rio.br (R. Sampaio).

http://dx.doi.org/10.1016/j.tws.2014.12.018
0263-8231/

shear-flexibility as well as warping effects due to non-uniform twisting were incorporated. These models were based on new theories for micro/macrostructures of composite materials, new modeling schemes including selective warping and second-order displacements, etc. The research of Wu and Sun [5], Librescu and coworkers [6,7], Kim et al. [8] and Cesnik et al. [9] are just a few examples of the most representative works in the modeling of composite beams with thin or thick walled cross-sections; however most of them were devoted to closed cross-sections as basic approaches for the analysis of helicopter blades. More recently Cortínez and Piovan [10] developed a theory of thin walled composite beams accounting for full shear flexibility (i.e. shear deformation due to bending as well as due to warping related to non-uniform twisting). The scopes and limits of the previous full shear flexible modeling conception were extended [11] by incorporating elastic couplings and the evaluation of general dynamic problems for straight beams and for curved thin-walled composite beams [12]. The model employed in this study was conceived in order to take into account the effects of shear deformability that are mandatory in the mechanics of thin-walled structures specially if they are constructed with fiber reinforced composite materials [6,8,10,12].

The behavior of composite structures under typical service in civil, aeronautical, aero-spatial or mechanical devices, is constrained to a number of factors that are stochastic in essence [13,14]. Many researchers have focused their attention in the evaluation of the stochastic response of composite structures since the middle 1990s [15,16]. Moreover, there is an increasing interest to quantify the propagation of uncertainty in the mechanics of composite materials at the microscale level [13] or for failure analysis [17]. The uncertainty involved in the material properties of the composites can be considered as random fields [18,19] among others. However, there are other ways for studying the dynamic response due to uncertainties in composite structures, for example by associating random variables to given entities that define a structural dynamic model. Effectively, when the parameters, such as material properties or reinforcement angles, are considered uncertain, the methodology for studying the uncertainty is called parametric probabilistic approach (PPA). However if the model as a whole is uncertain, the class of uncertainty is called systemic uncertainty. In order to analyze this type of uncertainty there are various approaches, one of them is the so-called non-parametric probabilistic approach (NPPA). The NPPA implies the introduction of random matrix variables. This approach was formulated by Soize [20] and employed in a variety of structural problems [21–23].

In this paper, the PPA and NPPA are applied in order to evaluate the uncertainty propagation in the dynamic response of naturally curved composite thin-walled beams. The theory for curved composite structures introduced by Piovan and Cortínez [12] is briefly revisited and employed as the nominal response or deterministic model in order to compare and quantify the uncertainty propagation of the stochastic approach. The solution of the dynamics equations is approximated in the context of the finite element method. For the PPA case, the parameters corresponding to elastic properties are considered uncertain. For the NPPA the stiffness matrix and the damping matrix are considered uncertain. This is due to the evidence gathered in other work of the authors [23] in which the elastic properties, and hence the stiffness matrix, are the main focus of uncertainty propagation in dynamics of composite thin-walled straight beams. To construct the probabilistic models, the probability density functions associated with the random variables are constructed appealing to the maximum entropy principle [24,25]. This principle uses the available information of the random entities to construct their probability density functions such that the entropy, in the sense of Shannon [26], is maximum. The use of this scheme allows the maximum possible propagation of the uncertainty according to the available information about the random variables.

The paper is organized as follows: after the introductory section where the state-of-the-art in modeling curved thin-walled composite beams is summarized, the deterministic/mean model and its finite element discretization are briefly described, then the probabilistic approach is constructed. The parametric and the non-parametric approaches are described for this problem and the subsequent section contains the computational studies, the analysis of the uncertainty propagation in the dynamics of thin-walled composite curved beams and finally concluding remarks are outlined.

2. Deterministic model

2.1. Brief description of the curved beam model

Fig. 1 shows a basic sketch of the structural component, in which it is possible to see the basic dimensions and the reference points $\boldsymbol{C}$ and $\boldsymbol{A}$. The principal reference point $\boldsymbol{C}$ is located at the geometric center of the cross-section, the x-direction is tangent to the curved axis of the beam, and y and z are the axes of the cross section, but not necessarily the principal axes of inertia. The secondary reference system, located at $\boldsymbol{A}$, is used to describe shell stresses and strains. The curved axis of the beam, that has constant radius R, is contained in the plane Ξ. The curved beam has an opening angle β and a circumferential length $L = R\beta$. The deterministic model of the present study is based on the following assumptions [11,12]:

1. The cross-section contour is rigid in its own plane (i.e. plane YZ).
2. The radius of curvature at any point of the shell is neglected.
3. The warping function is normalized with respect to the principal reference point $\boldsymbol{C}$.
4. A general laminate stacking sequence for a composite material is considered.
5. The material density is considered constant along the curved axis beam.
6. Stress and strain components are defined according to the secondary reference system located in $\boldsymbol{A}$.
7. The most representative stresses are σ_{xx}, σ_{xs} and σ_{xn}; and the most representative strain and curvature components are ϵ_{xx}, γ_{xs}, γ_{xn}, κ_{xx} and κ_{xs}.
8. The model is derived in the framework of linear elasticity.

Employing assumptions (1)–(7) one can derive the displacement field of the point $\boldsymbol{B}$ [12], which can be presented as follows:

$$\tilde{\mathbf{U}}_{\boldsymbol{B}} = \begin{Bmatrix} u_x \\ u_y \\ u_z \end{Bmatrix} = \begin{Bmatrix} u_{xc} - \omega\Phi_w \\ u_{yc} \\ u_{zc} \end{Bmatrix} + \begin{bmatrix} 0 & -\Phi_3 & \Phi_2 \\ \Phi_3 & 0 & -\Phi_1 \\ -\Phi_2 & \Phi_1 & 0 \end{bmatrix} \begin{Bmatrix} 0 \\ y \\ z \end{Bmatrix}, \quad (1)$$

where Φ_w, Φ_1, Φ_2 and Φ_3 are defined in terms of rotational and

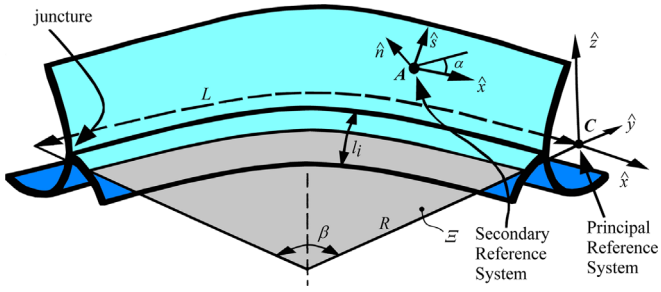

Fig. 1. Sketch of the thin-walled curved beam with the reference systems.

warping parameters as follows:

$$\Phi_1=\theta_x,\quad \Phi_2=\theta_y,\quad \Phi_3=\theta_z-\frac{u_{xc}}{R},\quad \Phi_w=\theta_w+\frac{\theta_y}{R} \tag{2}$$

and u_{xc}, u_{yc}, and u_{zc} are the displacements of the reference center in x-, y-, and z-directions, respectively. θ_z and θ_y are bending rotational parameters. θ_x is the twisting angle and θ_w is a warping-intensity parameter. R is the radius of curvature of the beam. In Eq. (1) the cross-sectional variables $y(s)$ and $z(s)$ of a generic point are related to the ones of the wall middle line $Y(s)$ and $Z(s)$ by means of Eq. (3) is the warping function normalized with respect to the reference center. It is defined in Eq. (4)

$$y(s)=Y(s)-n\frac{dZ}{ds},\quad z(s)=Z(s)+n\frac{dY}{ds}, \tag{3}$$

$$\omega(s,n)=\omega_p(s)+\omega_s(s,n). \tag{4}$$

In Eq. (4), $\omega_p(s)$ is the primary or contour warping function whereas $\omega_s(s,n)$ is the secondary or thickness warping. These entities are given by

$$\omega_p(s)=\int_s\left[r(s)+\psi(s)\right]ds-D_C,\quad \omega_s(s,n)=-nl(s), \tag{5}$$

where the functions $r(s)$, $l(s)$, $\psi(s)$ and D_C are defined in the following form (see Fig. 2):

$$r(s)=Z(s)\frac{dY}{ds}-Y(s)\frac{dZ}{ds},\quad l(s)=Y(s)\frac{dY}{ds}+Z(s)\frac{dZ}{ds},$$

$$\psi(s)=\frac{1}{\overline{A}_{66}(s)}\left[\frac{\int_s r(s)\,ds}{\oint_S\frac{1}{\overline{A}_{66}(s)}ds}\right],\quad D_C=\frac{\oint_S\left[r(s)+\psi(s)\right]\overline{A}_{11}(s)\,ds}{\oint_S\overline{A}_{11}(s)\,ds}. \tag{6}$$

The functions $\overline{A}_{11}$ and $\overline{A}_{66}$ are normal and tangential elastic coefficient of the composite laminates [11] which can vary along the section middle line. $\psi(s)$ is a function related to the torsional shear flow and D_C is a constant to normalize the warping function with respect to the reference system $\boldsymbol{C}$ [10,12]. The warping function is valid for both open and closed sections (since $\psi(s)=0$ in the case of open sections). Moreover the warping function described in Eq. (4) is conceptually analogous to the homonym warping function employed by Song and Librescu [7] but for composite straight beams.

The displacement–strain relations can be deduced by substituting Eq. (1) in the well-known expressions of linear strain components [1]. As it was shown by [12] the shell strains can be written as

$$\tilde{\mathbf{E}}_P=\frac{R}{R+y}\mathbf{G}_k\tilde{\mathbf{D}}, \tag{7}$$

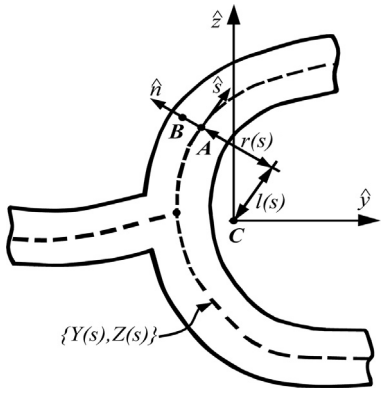

Fig. 2. Cross-section of the curved beam with the reference systems.

where

$$\tilde{\mathbf{E}}_P^T=\left\{\epsilon_{xx},\gamma_{xs},\gamma_{xn},\kappa_{xx},\kappa_{xs}\right\},$$

$$\tilde{\mathbf{D}}^T=\{\varepsilon_{D1},\varepsilon_{D2},\varepsilon_{D3},\varepsilon_{D4},\varepsilon_{D5},\varepsilon_{D6},\varepsilon_{D7},\varepsilon_{D8}\}, \tag{8}$$

$$\mathbf{G}_k=\begin{bmatrix}1 & Z & -Y & -\omega_p & 0 & 0 & 0 & 0\\ 0 & 0 & 0 & 0 & dY/ds & dZ/ds & r(s)+\psi(s) & -\psi(s)\\ 0 & 0 & 0 & 0 & -dZ/ds & dY/ds & l(s) & 0\\ 0 & -dY/ds & dZ/ds & -l(s) & 0 & 0 & 0 & 0\\ 0 & 0 & 0 & 0 & 0 & 0 & 1 & -2\end{bmatrix}. \tag{9}$$

In Eq. (8), ϵ_{xx}, γ_{xs} and γ_{xn} are the strain components and κ_{xx} and κ_{xs} are the curvatures of the shell that conforms the wall of the cross-section. These strain components are measured according to the wall reference system in $\boldsymbol{A}$. The entities ε_{Di}, $i=1,\ldots,8$ may be regarded as generalized deformations. In this context ε_{D1} is the axial deformation, ε_{D2} and ε_{D3} are bending deformations, ε_{D4} is the deformation due to non-uniform warping, ε_{D5} and ε_{D6} are the bending shear deformations, ε_{D7} is the warping shear deformation and finally ε_{D8} is the pure torsion shear deformation. These generalized deformations, which are collected in vector $\tilde{\mathbf{D}}$, are defined in the following form:

$$\tilde{\mathbf{D}}=\mathbf{G}_{DU}\tilde{\mathbf{U}}, \tag{10}$$

where $\mathbf{G}_{DU}$ is a matrix operator and $\tilde{\mathbf{U}}$ is the vector of kinematic variables which are defined in the following forms, in which $\partial_x(\diamond)$ is the spatial derivative operator

$$\mathbf{G}_{DU}=\begin{bmatrix}\partial_x(\diamond) & 1/R & 0 & 0 & 0 & 0 & 0\\ 0 & 0 & 0 & 0 & \partial_x(\diamond) & -1/R & 0\\ -\partial_x(\diamond)/R & 0 & \partial_x(\diamond) & 0 & 0 & 0 & 0\\ 0 & 0 & 0 & 0 & -\partial_x(\diamond)/R & 0 & \partial_x(\diamond)\\ 0 & \partial_x(\diamond) & -1 & 0 & 0 & 0 & 0\\ 0 & 0 & 0 & \partial_x(\diamond) & 1 & 0 & 0\\ 0 & 0 & 0 & 0 & 0 & \partial_x(\diamond) & -1\\ 0 & 0 & 0 & 0 & 1/R & \partial_x(\diamond) & 0\end{bmatrix}, \tag{11}$$

$$\tilde{\mathbf{U}}^T=\left\{u_{xc},u_{yc},\theta_z,u_{zc},\theta_y,\theta_x,\theta_W\right\}. \tag{12}$$

The principle of virtual works can be condensed in the following form:

$$\mathcal{W}_T=\int_L\left(\delta\tilde{\mathbf{D}}^T\tilde{\mathbf{S}}_R\right)dx+\int_L\delta\tilde{\mathbf{U}}^T\mathbf{M}_m\ddot{\tilde{\mathbf{U}}}\,dx-\int_L\delta\tilde{\mathbf{U}}^T\tilde{\mathbf{P}}_X\,dx+\delta\tilde{\mathbf{U}}^T\tilde{\mathbf{B}}_X\Big|_{x=0}^{x=L}=0, \tag{13}$$

where the vector of internal forces or, in other terms, generalized stress-resultants $\tilde{\mathbf{S}}_R$ is defined as follows:

$$\tilde{\mathbf{S}}_R^T=\left\{Q_x,M_y,M_z,B,Q_y,Q_z,T_w,T_{sv}\right\}, \tag{14}$$

whereas for the sake of fluid and clear reading, the matrix of mass coefficients $\mathbf{M}_m$, the vector of external forces $\tilde{\mathbf{P}}_X$ and the vector of natural boundaries conditions $\tilde{\mathbf{B}}_X$ are detailed in Appendix A. Q_x, M_y, M_z, and B identify the axial force, the bending moment in the y-direction, the bending moment in the z-direction, and the bi-moment, respectively; whereas Q_y, Q_z, T_w, and T_{sv} correspond to the shear force in the y-direction, the shear force in the z-direction, the twisting moment due to warping and the twisting moment due to pure torsion, respectively. These internal/generalized forces can be written in terms of the shell-forces as [11]

$$\tilde{\mathbf{S}}_R=\int_S\mathbf{G}_k^T\tilde{\mathbf{N}}_P\,ds, \tag{15}$$

where $\tilde{\mathbf{N}}_P$ is the vector of shell stress resultants or shell forces and moments defined according to [1,2]

$$\tilde{\mathbf{N}}_P^T = \int_S \{\sigma_{xx}, \sigma_{xs}, \sigma_{xn}, n\sigma_{xx}, n\sigma_{xs}\}\, dn. \tag{16}$$

The differential equations of motion and corresponding boundary conditions are derived by applying variational procedures in Eq. (13). The differential equations of motion can be useful for some numerical methods, e.g. power series method or differential quadrature. While in the present paper the finite element method is employed, the derivation of differential equations is not necessary. The interested readers may follow in the technical literature authors' articles [12,27] devoted to evaluate the differential equations of the thin-walled curved beam model applied to a number of specific structural problems.

2.2. Constitutive equations in terms of internal forces and generalized strains

In order to obtain the relationship between beam stress resultants and generalized deformations ε_{D_i}, $i=1,\ldots,8$, one has to select the constitutive laws for a composite shell and use appropriate constitutive hypotheses [12] of the shell stress resultants in terms of the shell strains. The shell stress resultants can be expressed in terms of the generalized deformations defined in Eq. (10) according to the following matrix form:

$$\tilde{\mathbf{N}}_P = \mathbf{M}_C \tilde{\mathbf{E}}_P, \tag{17}$$

where $\mathbf{M}_C$ is the matrix of modified shell stiffness, which depends on the type of constitutive hypotheses involved [12,23,27] and can be expressed in the following form:

$$\mathbf{M}_C = \begin{bmatrix} \overline{A}_{11} & \overline{A}_{16} & 0 & \overline{B}_{11} & \overline{B}_{16} \\ & \overline{A}_{66} & 0 & \overline{B}^*_{16} & \overline{B}_{66} \\ & & \overline{A}^*_{55} & 0 & 0 \\ & \text{sym} & & \overline{D}_{11} & \overline{D}_{16} \\ & & & & \overline{D}_{66} \end{bmatrix}. \tag{18}$$

The elastic stiffness coefficients $\overline{A}_{11}$, $\overline{B}_{11}$, $\overline{D}_{11}$, etc., are not described in the present paper, however the interested readers can find their definition and "in-extenso" expressions in the authors' previous works [12,27].

Substituting Eq. (17) into Eq. (15) the curved beam stress resultants can be represented in terms of generalized strains as

$$\tilde{\mathbf{S}}_R = \mathbf{M}_k \tilde{\mathbf{D}}, \tag{19}$$

where

$$\mathbf{M}_k = \int_S \mathbf{G}_k^T \mathbf{M}_C \mathbf{G}_k\, ds. \tag{20}$$

The matrix $\mathbf{M}_k$ of cross-sectional stiffness coefficients leads to constitutive elastic coupling or not, depending on the stacking sequence of the laminates in a given cross-section. The interested reader can follow an extended explanation about elastic constitutive coupling in the books of Barbero [1] and Jones [2]. Moreover for beam applications the explanation of the constitutive coupling can be followed in the works of Piovan and Cortínez [12] and Kim et al. [8], among others.

2.3. Finite element approach

In order to perform the calculations, the curved beam model is discretized with iso-parametric elements of five nodes per element, seven degrees-of-freedom per node and shape functions of quartic order. The formulation of the finite element approach for this type of curved structural member has been introduced in previous works [12] in which the interested readers can find detailed explanations. The assembled finite element equation can be written in the conventional form as

$$\mathbf{K}\overline{\mathbf{W}} + \mathbf{C}\dot{\overline{\mathbf{W}}} + \mathbf{M}\ddot{\overline{\mathbf{W}}} = \overline{\mathbf{F}}, \tag{21}$$

where $\mathbf{K}$ and $\mathbf{M}$ are the global matrices of elastic stiffness and mass, respectively; whereas $\overline{\mathbf{W}}$, $\ddot{\overline{\mathbf{W}}}$ and $\overline{\mathbf{F}}$ are the global vectors of nodal displacements, nodal accelerations and nodal forces, respectively. The damping in Eq. (21) is incorporated as an "a posteriori" procedure after the discretization of the functional given in Eq. (13). Then $\mathbf{C}$ identifies the global matrix of structural damping, calculated according to Rayleigh's definition as

$$\mathbf{C} = \eta_1 \mathbf{M} + \eta_2 \mathbf{K}. \tag{22}$$

The coefficients η_1 and η_2 in Eq. (22) are computed by using the damping coefficients, ξ_1 and ξ_2, according to the common methodology presented in the bibliography related to finite element procedures [28].

The response in the frequency domain of the linear dynamic system given by Eq. (21) can be written as

$$\widehat{\mathbf{W}}(\omega) = \left[-\omega^2\mathbf{M} + i\omega\mathbf{C} + \mathbf{K}\right]^{-1} \widehat{\mathbf{F}}(\omega), \tag{23}$$

where $\widehat{\mathbf{W}}$ and $\widehat{\mathbf{F}}$ are the Fourier transform of the displacement vector and force vector, respectively; whereas ω is the circular frequency measured in (rad/s).

2.4. Reduced order model

The calculation of the responses in the frequency domain is normally quite demanding in terms of computational cost. Then, in order to have a speedup in the calculation process, it is mandatory to construct a reduced model by defining an appropriate projection basis. Thus, taking advantage of the linearity of the present formulation, the projection basis for the reduced model can be extracted from the following eigenvalue problem:

$$\omega_i^2 \mathbf{M}\overline{v}_i = \mathbf{K}\overline{v}_i, \tag{24}$$

where ω_i^2 and $\overline{v}_i$ are the square of the ith natural frequency and its corresponding eigenvector.

Now, defining the global vector of kinematic variables $\overline{\mathbf{W}}$ in terms of the projection basis $\mathbf{V}$ and the modal coordinates $\overline{\mathbf{Q}}$:

$$\overline{\mathbf{W}} = \mathbf{V}\overline{\mathbf{Q}}, \tag{25}$$

and using it in Eq. (21) according to the common procedure of model reduction [29] it is possible to write the following expression:

$$\mathbf{K}_r\overline{\mathbf{Q}} + \mathbf{C}_r\dot{\overline{\mathbf{Q}}} + \mathbf{M}_r\ddot{\overline{\mathbf{Q}}} = \overline{\mathbf{F}}_r, \tag{26}$$

and finally

$$\widehat{\mathbf{W}}(\omega) = \mathbf{V}\widehat{\mathbf{Q}}(\omega) = \left[-\omega^2\mathbf{M}_r + i\omega\mathbf{C}_r + \mathbf{K}_r\right]^{-1} \widehat{\mathbf{F}}_r(\omega). \tag{27}$$

In the previous expressions the following definitions have been used:

$$\begin{aligned} \mathbf{M}_r &= \mathbf{V}^T\mathbf{M}\mathbf{V} \\ \mathbf{C}_r &= \mathbf{V}^T\mathbf{C}\mathbf{V} \\ \mathbf{K}_r &= \mathbf{V}^T\mathbf{K}\mathbf{V} \\ \mathbf{F}_r &= \mathbf{V}^T\mathbf{F}. \end{aligned} \tag{28}$$

Notice that $\mathbf{V}$ is a $(n \times m)$ matrix whose columns correspond to the m eigenvectors selected to reduce the model.

Models of 12 finite elements (i.e. 343 degrees of freedom) are employed to do the calculations. This number of elements is enough to reach approximation errors less than 1% up to the 8-th frequency. Moreover with 24 normal modes one reaches a mean error less than 0.1% in the frequency response functions. This

implies a reduction of about 92% in size that was reflected in a calculation procedure, at least, 150 times faster.

3. Description of the probabilistic model

The probabilistic model is constructed by selecting parameters or matrices as uncertain entities and then deducing the appropriate and corresponding random variables based on the available information. Whether it is employed the PPA or the NPPA, the probabilistic approach is constructed from the finite element equation of the deterministic model which is assumed as the mean model. The construction of the probabilistic model is quite sensitive in the analysis of uncertainty propagation. This involves the deduction of the probability density functions of the random entities (parameters or matrices depending on the selected approach) taking into account the scarce information about the random entities. According to the authors' opinion, the use of the maximum entropy principle (MEP) allows the construction of a probabilistic model despite the lack of information about the random variables. In this context, the probability density functions of the random variables can be derived guaranteeing consistence with the available information and the physics of the problem.

In order to derive the probability density functions of the random variables, the maximum entropy principle is proposed in the following form:

$$p_V^{(opt)} = \arg\max_{p_V \in \mathfrak{P}} S(p_V) \tag{29}$$

where $p_V^{(opt)}$ is the optimal probability density function such that $S(p_V^{(opt)}) \geq S(p_V)$, $\forall p_V \in \mathfrak{P}$, and S is the measure of entropy whereas $\mathfrak{P}$ is a set of admissible probability density functions satisfying the known data of the random variables and the physical constraints. The measure of the entropy S is defined as [26]

$$S(p_V) = -\int_{\mathfrak{S}} p_V \ln(p_V)\, dv \tag{30}$$

where $\mathfrak{S}$ is the support of the probability distributions of the random variables taken into account in the optimization procedure.

Once the random variables are appropriately defined then the stochastic finite element equation can be written, through Eq. (23), in the following form:

$$\widehat{\mathbb{W}}(\omega) = \mathbf{V}\widehat{\mathbb{Q}}(\omega) = \left[-\omega^2\mathbf{M}_r + i\omega\mathbb{C}_r + \mathbb{K}_r\right]^{-1}\widehat{\mathbf{F}}_r(\omega). \tag{31}$$

Notice that in Eq. (31) the math-blackboard typeface indicates stochastic entities, thus the stiffness matrix $\mathbb{K}_r$ is stochastic because random variables (scalars or matrices) are employed in its construction, and the damping matrix $\mathbb{C}_r$ is stochastic through the stochastic nature of $\mathbb{K}_r$ in Eq. (22), hence $\widehat{\mathbb{W}}$ is stochastic.

The Monte Carlo method is used for the simulation of the stochastic dynamics. This strategy leads to the calculation of a deterministic system for each realization of the random variables employed. The convergence of the stochastic response $\widehat{\mathbb{W}}$ can be calculated with the following function:

$$\mathrm{conv}(N_{MS}) = \sqrt{\frac{1}{N_{MS}}\sum_{j=1}^{N_{MS}}\int_{\Omega} \|\,\widehat{\mathbb{W}}_j(\omega) - \widehat{\mathbf{W}}(\omega)\,\|^2\, d\omega}, \tag{32}$$

where N_{MS} is the number of Monte Carlo samplings and Ω is the frequency band of analysis. Clearly, $\widehat{\mathbb{W}}$ is the response of the stochastic model and $\widehat{\mathbf{W}}$ is the response of the mean model or deterministic model.

3.1. Parametric approach

The stochastic model according to the PPA is constructed selecting two sets of uncertain parameters and associating random variables to them. One set for the orientation angles of the fiber reinforcement in the layers of each panel and other set for basic elastic properties of the material. In the present problem random variables V_i, $i = 1, 2 \ldots N_P$ and V_i, $i = N_P+1, \ldots, N_P+6$ are introduced such that they represent the angles of N_P different plies in a cross-sectional laminate and the basic elastic properties of the material (i.e. elastic moduli: E_{11}, $E_{22} = E_{33}$, $G_{12} = G_{13}$ and G_{23}, Poisson coefficients: $\nu_{12} = \nu_{13}$ and ν_{23}), respectively.

The available information to deduce the probability density functions is associated with some information that can be found in the technical literature [13]. The following conditions are proposed in order to construct the probability density functions with the maximum entropy principle:

- The random variables associated with material properties are positive and have bounded supports.
- The random variables associated with the reinforcement angles have bounded supports whose upper and lower limits are distant Δ_α from the expected value $\underline{V}_i$.
- The expected values are $\mathcal{E}\{V_i\} = \underline{V}_i$, $i = 1, \ldots N_P+6$, i.e. those corresponding to the deterministic model.
- The variance of the random variable has to be kept finite in order to satisfy the physical consistence of the problem.
- There is no information about the correlation between random variables.

Consequently, according to the aforementioned background, the probability density functions of the random variables V_i can be written as

$$p_{V_i}(v_i) = \mathfrak{S}_{\left[\mathcal{L}_{V_i}, \mathcal{U}_{V_i}\right]}(v_i)\frac{1}{2\Delta_\alpha}, \quad i = 1, \ldots, N_P \tag{33}$$

$$p_{V_i}(v_i) = \mathfrak{S}_{\left[\mathcal{L}_{V_i}, \mathcal{U}_{V_i}\right]}(v_i)\frac{1}{2\sqrt{3}\underline{V}_i\delta_{V_i}}, \quad i = N_P+1, \ldots, N_P+6 \tag{34}$$

where $\mathfrak{S}_{\left[\mathcal{L}_{V_i}, \mathcal{U}_{V_i}\right]}(v_i)$ is the generic support function, whereas $\mathcal{L}_{V_i}$ and $\mathcal{U}_{V_i}$ are the lower and upper bounds of the random variable V_i. Δ_α is a gap measured in angular units (radians or degrees), whereas δ_{V_i} is the coefficient of variation. The Matlab [30] function unifrnd $\left(\underline{V}_i - \Delta_\alpha, \underline{V}_i + \Delta_\alpha\right)$ can be used to generate realizations of the random variables V_i, $i = 1, 2 \ldots N_P$. The Matlab function unifrnd $\left(\underline{V}_i\left(1 - \delta_{V_i}\sqrt{3}\right), \underline{V}_i\left(1 + \delta_{V_i}\sqrt{3}\right)\right)$ can be used to generate realizations of the random variables V_i, $i = N_P+1, \ldots, N_P+6$.

3.2. Non-parametric approach

Under this conception, the matrices of the system are considered uncertain. In particular, there is evidence [23] that the uncertainty in the elastic properties is more sensitive than the uncertainty in the mass properties in the dynamics of beams constructed with composite materials. Consequently, the construction of the probability density function of the random stiffness matrix $\mathbf{K}$ is performed in this section. The procedure explained in the subsequent lines follows the concepts and ideas elaborated in the works [31,20,32].

In order to construct the random matrix $\mathbb{K}$, it is necessary that the mean value (or the deterministic one) of the positive-definite matrix $\mathbf{K}$ to be written according to the Cholesky-decomposition, that is $\mathbf{K} = \mathbf{L}_\mathbf{K}^T\mathbf{L}_\mathbf{K}$, where $\mathbf{L}_\mathbf{K}$ is an upper triangular matrix. Hence the random matrix $\mathbb{K}$ can be written as follows:

$$\mathbb{K} = \mathbf{L}_\mathbf{K}^T\mathbb{G}\mathbf{L}_\mathbf{K} \tag{35}$$

where $\mathbb{G}$ is a random matrix that has the following constraints:

- Positive-definiteness.
- The mean value is the identity matrix: $\mathcal{E}\{\mathbb{G}\} = \mathbf{I}$.

- The mean square value of its inverse is finite, i.e $\mathcal{E}\left\{\|\mathbb{G}^{-1}\|_F^2\right\} < +\infty$; this assures that the response of the system is a second-order random variable.

Then using the maximum entropy principle the probability density function of $\mathbb{G}$ can be written as [31]

$$p_{\mathbf{G}}(\mathbf{G}) = \mathfrak{S}_{\mathbb{M}^+(\mathbb{R})}(G) C_{\mathbb{G}} \det(\mathbf{G})^{(n+1)((1-\delta_{\mathbb{K}}^2)/2\delta_{\mathbb{K}}^2)} \exp\left\{-\frac{n+1}{2\delta_{\mathbb{K}}^2}\mathrm{tr}(\mathbf{G})\right\} \tag{36}$$

where $\mathfrak{S}_{\mathbb{M}^+(\mathbb{R})}(G)$ is the support of the random variable, n is the dimension of the random matrix $\mathbb{G}$, the dispersion parameter $\delta_{\mathbb{K}}$ and $C_{\mathbb{G}}$ are given as follows:

$$\delta_{\mathbb{K}} = \sqrt{\frac{1}{n}E\left\{\|\mathbb{G}-\mathbf{I}\|_F^2\right\}}, C_{\mathbb{G}} = \frac{(2\pi)^{(n-n^2)/4}\left(\frac{n+1}{2\delta_{\mathbb{K}}^2}\right)^{(n+n^2)/\left(2\delta_{\mathbb{K}}^2\right)}}{\prod_{j=1}^{n}\Gamma\left(\frac{n+1}{2\delta_{\mathbb{K}}^2}+\frac{1-j}{2}\right)} \tag{37}$$

The dispersion parameter is such that $0 < \delta_{\mathbb{K}} < \sqrt{(n+1)/(n+5)}$, where n is the number of degrees of freedom.

Thus, for each realization of the random matrix $\mathbb{K}$, the matrix $\mathbb{G}$ is built by means of a Cholesky decomposition, i.e. $\mathbb{G} = \mathbb{L}^T\mathbb{L}$, where $\mathbb{L}$ is an upper triangular positive-definite random matrix subjected to the following constraints:

- The random variables $\{\mathbb{L}_{jk}, j \le k\}$ are independent.
- For $j < k$, the real-valued random variable $\mathbb{L}_{jk} = \sigma V_{jk}$, in which $\sigma = \delta_{\mathbb{K}}\sqrt{n+1}$ and V_{jk} is a real-valued random variable with zero mean and unit variance.
- For $j = k$ the real-valued random variable $\mathbb{L}_{jk} = \sigma\sqrt{2V_j}$, in which V_j is a real-valued gamma random variable with probability density function:

$$p_{V_j}(v) = \mathfrak{S}_{\mathbb{R}^+}(v)\frac{v^{\left(\frac{n+1}{2\delta_{\mathbb{K}}^2}-\frac{1-j}{2}\right)}}{\Gamma\left(\frac{n+1}{2\delta_{\mathbb{K}}^2}+\frac{1-j}{2}\right)}\exp(v) \tag{38}$$

As it is possible to infer, the random variables $V_{jk}, j \neq k$ and $V_{jk}, j = k$ can be generated by a normal distribution and a gamma distribution respectively. In fact they can be generated in the Monte Carlo simulation procedure by means of the Matlab functions normrnd$(0,1)$ and gamrnd(α,β), with $\alpha = \left(((n+1)/2\delta^2)+((1-j)/2)\right)$ and $\beta = 1$.

4. Computational studies

4.1. Definitions and convergence checks

In this section a study is carried out related to the propagation of uncertainties due to material properties and/or constructive aspects of composite laminates, in the dynamic response of curved thin-walled composite beams. For this study a curved beam (length $L = 6.0$ m, radius $R = 6.0$ m) with rectangular cross-section is employed. The following Fig. 3 shows the rectangular cross-section with the secondary reference systems associated to each panel. Moreover it is possible to see the excitation due to an impulsive unitary force located at $\mathbf{U_B} = \{\mathbf{x},\mathbf{y},\mathbf{z}\} = \{\mathbf{x}_B, \mathbf{b}/\mathbf{2}, \mathbf{h}/\mathbf{2}\}$ and oriented with $\psi = 45^o$, where $x_B = L$ in a clamped–free boundary condition or $x_B = L/2$ if the boundary condition is doubly-clamped. The web height and flange width are $h = 0.6$ m and $b = 0.3$ m, respectively, whereas the thickness of all laminates is $e = 0.03$ m. Each laminate is composed by eight

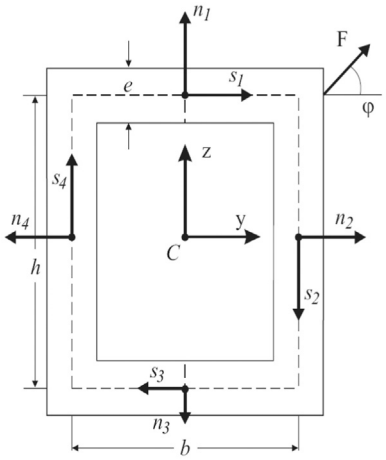

Fig. 3. Rectangular cross-section with reference systems.

Table 1
Lamination schemes for the cross-sections.

Cross-section	Laminate name	Angle orientation
□	CUS(α)	Left and right panels: $\{(\alpha,\alpha)_4\}$ Upper and lower panels: $\{(\alpha,\alpha)_4\}$
	CAS(α)	Upper and right panels: $\{(\alpha,\alpha)_4\}$ Lower and left panels: $\{(-\alpha,-\alpha)_4\}$
	CUS(0|α)	Left and right panels: $\{(0,\alpha)_4\}$ Upper and lower panels: $\{(0,\alpha)_4\}$
	CAS(0|α)	Upper and right panels: $\{(0,\alpha)_4\}$ Lower and left panels: $\{(0,-\alpha)_4\}$

laminas of equal thickness. The material of the beams is graphite-epoxy (AS4/3501-6) whose properties are $E_{11} = 144$ GPa, $E_{22} = E_{33} = 9.68$ GPa, $G_{12} = G_{13} = 4.14$ GPa, $G_{23} = 3.45$ GPa, $\nu_{12} = \nu_{13} = 0.3$, $\nu_{23} = 0.5$, and the density $\rho = 1389$ kg/m^3. Although the damping coefficients could be uncertain, in this study they assume fixed values $\xi_1 = 0.05$ and $\xi_2 = 0.05$ in order to facilitate the analysis of uncertainty connected with elastic properties and the modeling itself.

The stacking sequences to be used are described in Table 1, in which the acronyms CUS and CAS stand for "circumferential uniform stiffness" and 'circumferential asymmetric stiffness". These acronyms were introduced by [33] to identify a particular type of lamination scheme, and hence elastic coupling, for rectangular cross-sections. The CUS laminate corresponds to elastic constitutive coupling between twisting moments and axial force as well as both shear forces and both bending moments; whereas the CAS laminate leads to elastic constitutive coupling between bending moments and twisting moments together with coupling of the axial force with both shear forces [8,11,33].

The cases CAS(0) and CUS(0) are the same or imply the same coupling as well as the cases CAS(90|0) and CUS(90|0). In these last cases there is no constitutive elastic coupling between all the kinematic variables. In these circumstances the system of seven equations can be decoupled into two subsets of equations [12]: namely for in-plane motions (u_{xc}, u_{yc}, θ_z) and for out-of-plane motions (u_z, θ_y, θ_x, θ_w).

It is interesting, for further comparative purposes, to recall not only the type of constitutive elastic coupling but also the ratio between effective longitudinal stiffness ($\overline{A}_{11}$) and shear membranal ($\overline{A}_{66}$) and transverse shear stiffness ($\overline{D}_{66}$). Thus, for the material and laminations selected, in Table 2 the ratio of some elastic properties is shown. As it may be observed, the ratios decrease as the laminate contains more layers with angle of

reinforcement away of the orthotropic directions (i.e. at $\alpha=0^\circ$ and $\alpha=90^\circ$). Although the ratios $\overline{A}_{11}/\overline{A}_{66}$ and $\overline{A}_{11}/\overline{D}_{66}$ have the same value for CAS and CUS configurations, it is important to recall that the global elastic behavior in the structure is quite different as it is mentioned above.

The stochastic analysis of the present study is mainly concerned with the evaluation of the uncertainty propagation in the frequency response function of the composite curved beam subjected to a unit force F that perturbs the structure. The response is observed at the location of the forcing point and evaluated by means of the following frequency response function:

$$H_F(\omega)=\frac{\|\widehat{\mathbf{U}}_{\boldsymbol{B}}(\omega)\|}{\widehat{F}(\omega)}. \tag{39}$$

In Eq. (39), $\|\widehat{\mathbf{U}}_{\boldsymbol{B}}\|$ is the norm of the Fourier transform of the displacement vector of the point in which the force is applied (see Fig 3) and $\widehat{F}$ is the Fourier transform of the force applied at the beam's end. Moreover, the following frequency response functions are introduced for specific comparative purposes:

$$H_1(\omega)=\frac{\widehat{u}_{yc}(\omega)}{\widehat{F}_y(\omega)},\quad H_2(\omega)=\frac{\widehat{u}_{zc}(\omega)}{\widehat{F}_z(\omega)},\quad H_3(\omega)=\frac{\widehat{\theta}_x(\omega)}{\widehat{T}_x(\omega)}, \tag{40}$$

where $\widehat{u}_{yc}$, $\widehat{u}_{zc}$ and $\widehat{\theta}_x$ are the Fourier transforms of lateral displacement, vertical displacement and twisting angle, respectively, whereas $\widehat{F}_y$, $\widehat{F}_z$ and $\widehat{T}_x=\widehat{T}_w+\widehat{T}_{sv}$ are the Fourier transforms of the components of force F and the associated twisting moment. For this problem, the displacements are calculated at the free end.

In the PPA, four random variables are selected to identify the orientation angles of the fiber reinforcement according to the common stacking sequences employed in the construction of composite structures. These random variables have the following expected values: $\mathcal{E}\{V_1\}=0^\circ$, $\mathcal{E}\{V_2\}=15^\circ$, $\mathcal{E}\{V_3\}=45^\circ$ and $\mathcal{E}\{V_4\}=90^\circ$, with $\Delta_\alpha\in[2^\circ,4^\circ]$. On the other hand the expected values of random variables V_i, $i=5,\ldots,10$ correspond to the nominal values of the elastic properties indicated above. The elastic random variables can have dispersion parameters contained in $\delta_i\in[0.04,0.12]$, $i=5,\ldots,10$ [13,23].

Recall that the discrete models contain 12 finite elements, and it should be noted that a clamped end restricts the motion of the seven kinematic variables. This implies that depending on the case of clamped–free or double clamped beam, $n=336$ or $n=329$ should be used in Eq. (37). In the case of the NPPA it is important to identify the limits of the dispersion parameter that according to Section 3.2 it should be, for example: $0<\delta_{\mathbb{K}}<\sqrt{(336+1)/(336+5)}=0.9941$ in the case of a clamped–free beam (and $0<\delta_{\mathbb{K}}<0.9939$ in the case of a double-clamped beam). The uncertainty dispersion parameter in the NPPA can take the following values: $\delta_{\mathbb{K}}\in[0.20,0.50,0.65,0.80,0.95]$. In fact the lower value implies a model with a slight global uncertainty and the higher value indicates a model with strong uncertainty.

Fig. 4 shows two examples of the convergence in the Monte Carlo simulations performed according to the PPA and NPPA of a clamped–free beam. In both cases the evolutions of the function conv(N_{MS}) is evaluated with respect to the number of simulations. The cross-section has a stacking sequence CAS(15) with the following parameters: $\Delta_\alpha=4^\circ$ and $\delta_i=0.1, i=1,\ldots,N_P+6$ for the PPA and $\delta_{\mathbb{K}}=0.9$ for the NPPA. It can be seen that with nearly 300 simulations, the conv(N_{MS}) function reaches an acceptable level of convergence. The convergence has been controlled for each simulation performed in the subsequent studies of uncertainty propagation.

Table 2
Ratios $\overline{A}_{11}/\overline{A}_{66}$ and $\overline{A}_{11}/\overline{D}_{66}$ for different stacking sequences.

Laminate name	$\overline{A}_{11}/\overline{A}_{66}$	$\overline{A}_{11}/\overline{D}_{66}$
CUS(0) or CAS(0)	34.78	417.39
CUS(0|90) or CAS(0|90)	18.64	223.74
CUS(0|15) or CAS(0|15)	16.20	194.42
CUS(15) or CAS(15)	9.82	117.92
CUS(0|45) or CAS(0|45)	8.02	96.33
CUS(45) or CAS(45)	1.31	15.79

4.2. A brief discussion on the uncertainty in the formulation of shear flexibility

The appropriate way to model the shear flexibility and its effect in the mechanics of slender composite structures was an interesting problem that attracted the attention of many researchers [1,7,10,34,35]. The discussion has been focused in the appropriate way of incorporating the thickness shear deformation, i.e. γ_{xn} of Eq. (7). In some models (Bauchau [4] and Wu and Sun [5] for example), γ_{xn} has been neglected and in other contemporary models it was included (Librescu and Song [6], as the remarkable

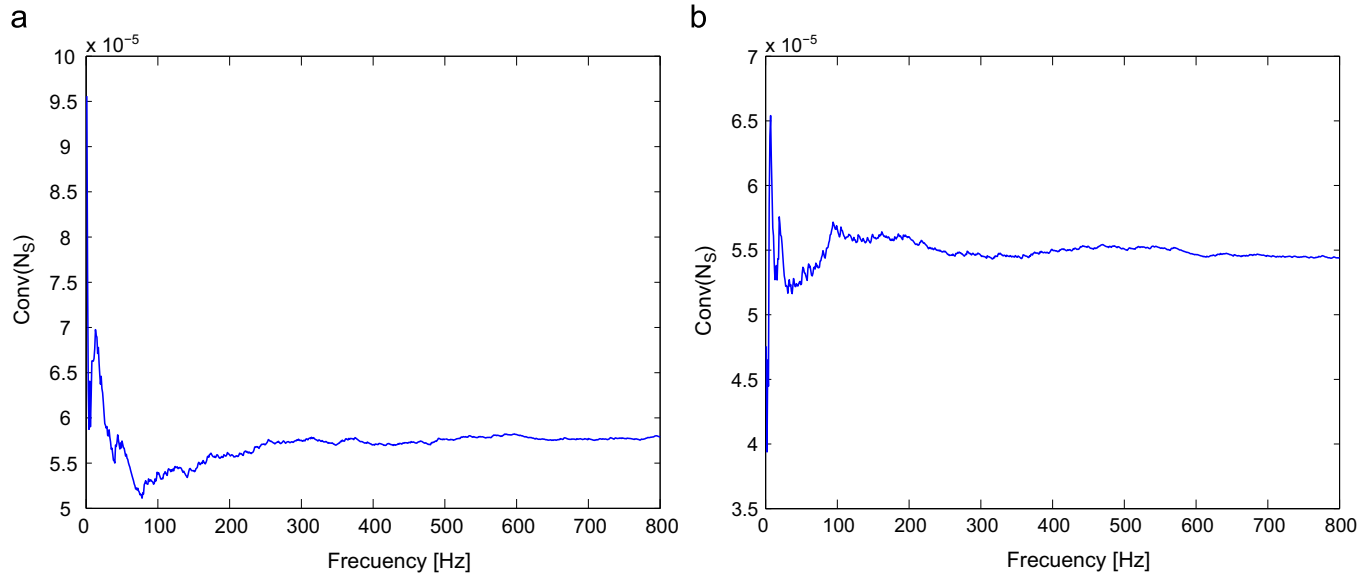

Fig. 4. Convergence of the Monte Carlo simulations for CAS(15). (a) PPA with $\Delta_\alpha=4^\circ$ and $\delta_i=0.1$, (b) NPPA with $\delta_{\mathbb{K}}=0.9$.

case). The controversy has been discussed [10,34,36] by comparing the responses of the conventional 1D models with a number of advanced models (finite element 2D and 3D formulations or even enhanced 1D formulations). From these studies, it was clear that, for static problems, the incorporation of thickness shear deformation does not affect the sensitivity of the response. However, for dynamic problems, the response can be seriously affected depending on the case of stacking sequence, ratio thickness to flanges width, among others; and the incorporation of the thickness shear is discouraged.

Nevertheless, these aspects may be also evaluated and quantified in the frame of the uncertainty of the model. Thus as a first comparative study two classes of stacking sequences are taken into account; one corresponds to an extreme orthotropic laminate, e.g. CAS(0), and the other to a more balanced laminate, but certainly not isotropic, e.g. CAS(45) or CUS(45). The deterministic FRFs of the models taking into account $\gamma_{xn}=0$ and $\gamma_{xn}\neq 0$ are calculated and contrasted with the bounds of the Monte Carlo simulation performed with modeling uncertainty $\delta_{\mathbb{K}}$ based in a deterministic model where thickness shear deformation is neglected.

In Fig. 5(a) the FRFs of the clamped–free beams with CAS(45) and CUS(45) with $\delta_{\mathbb{K}}=0.4$ are shown. The bounds of the Monte Carlo simulation are also depicted. Now in Fig. 5(b) the FRFs of a clamped–clamped beams with $\delta_{\mathbb{K}}=0.99$ are depicted. Notice that, in the case of a lamination CAS(45) or CUS(45), the FRFs of the deterministic models accounting or not for thickness shear deformation are contained inside the bounds of the stochastic model with the corresponding level of uncertainty. However in the case of the stacking sequence CUS(0) neither with the maximum level of uncertainty in the stochastic model (i.e. $\delta_{\mathbb{K}}=0.99$) both the deterministic approaches can be contained inside the bounds of the Monte Carlo simulations of the probabilistic model. Moreover the cases of CAS(45) or CUS(45) can be considered within the modeling uncertainty of $\delta_{\mathbb{K}}=0.4$ until the fourth frequency, and the case of CUS(0)/CAS(0) even in the allowable maximum level of uncertainty of $\delta_{\mathbb{K}}=0.99$ the first frequency can be clearly attainted.

In order to identify bounds of uncertainty in the model due to the thickness shear deformability the following Table 3 is presented. In this table it is summarized the value of $\delta_{\mathbb{K}}$ in the NPA whose realization bounds can cover the 100% of the FRFs of both the deterministic models (with and without thickness shear deformability); moreover it is included in the order of the frequency where the FRFs fall out the simulation bounds. In some cases, e.g. CUS(0)/CAS(0) with double clamped boundary conditions, where there is extreme uncertainty, reaching nearly the maximum level of uncertainty allowable for the model of finite elements, as it is seen in Fig. 5(b).

As one can see in Table 3 the structures with more orthotropic laminates and more rigid boundary conditions are more sensitive to the modeling uncertainty, and the laminates with the lower values in the ratios: $\overline{A}_{11}/\overline{A}_{66}$ and $\overline{A}_{11}/\overline{D}_{66}$ are less sensitive to uncertainties. In general the stiffness criteria of incorporating the thickness shear deformability leads to a stiffening of the dynamic responses, shifting the FRFs to the right.

4.3. Uncertainty propagation in the dynamics of curved composite beams

In this section the propagation of uncertainty in the dynamics of curved thin-walled composite beams is evaluated in different cases of stacking sequences and boundary conditions and the parametric and non-parametric approaches are compared as well. Taking into account the conclusions of the previous paragraph and in view of the discussion about the disadvantages in incorporating the thickness shear deformation in the transient dynamic analysis of composite structures [34,35], in the subsequent calculations the thickness shear deformation (γ_{xn}) is neglected in the constitutive formulation.

Thus as a first study, a clamped–free curved beam with the lamination scheme CAS(15) is selected. Now, Fig. 6 shows the frequency response functions of the simulation in which the PPA has been employed. In Fig. 6(a) the dispersion parameter of the elastic

Table 3
Quantification of the level of uncertainty $\delta_{\mathbb{K}}$ due to thickness shear deformation of some stacking sequences and boundary conditions.

Laminate	*Clamped–free*		*Clamped–clamped*	
name	$\delta_{\mathbb{K}}$	Order freq.	$\delta_{\mathbb{K}}$	Order freq.
CUS(0)/*CAS*(0)	0.80	1	0.99	0
CUS(0|90)/*CAS*(0|90)	0.62	1	0.95	1
CUS(0|15)	0.60	2	0.85	1
CUS(0|45)	0.45	2	0.70	1
CUS(45)/*CAS*(45)	0.40	4	0.48	3

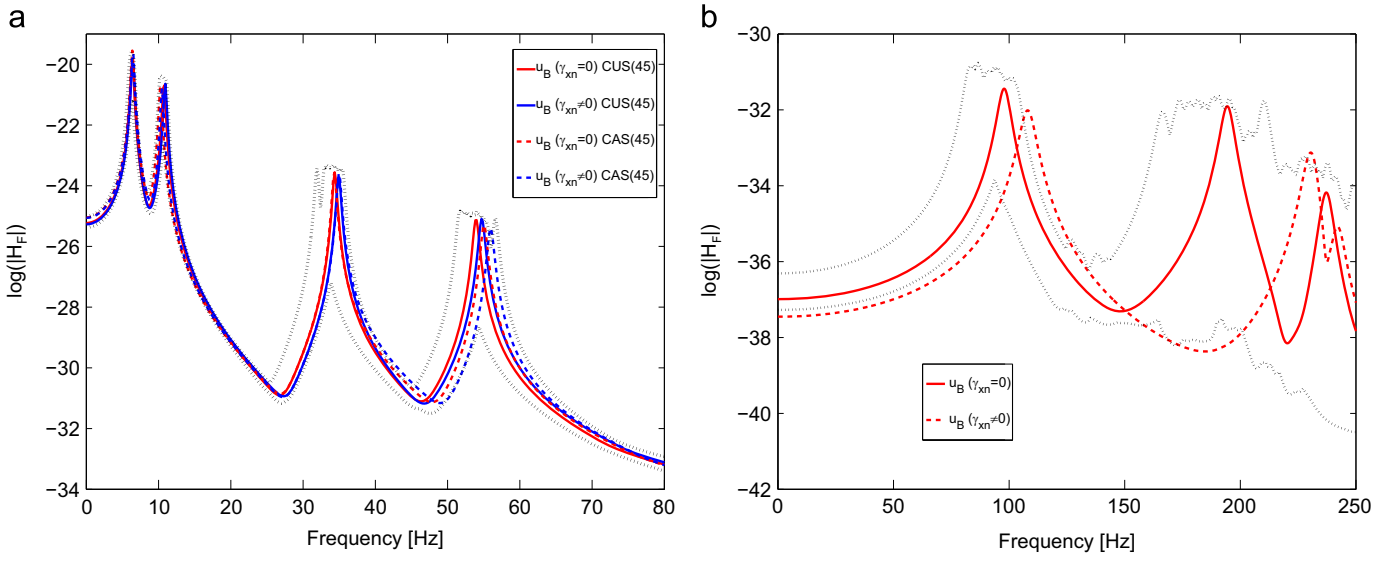

Fig. 5. Responses with and without thickness shear deformation γ_{xn}. (a) Clamped–free beam with CAS(45) and CUS(45) and $\delta_{\mathbb{K}}=0.3$. (b) Clamped–clamped beam with CUS(0) and $\delta_{\mathbb{K}}=0.99$.

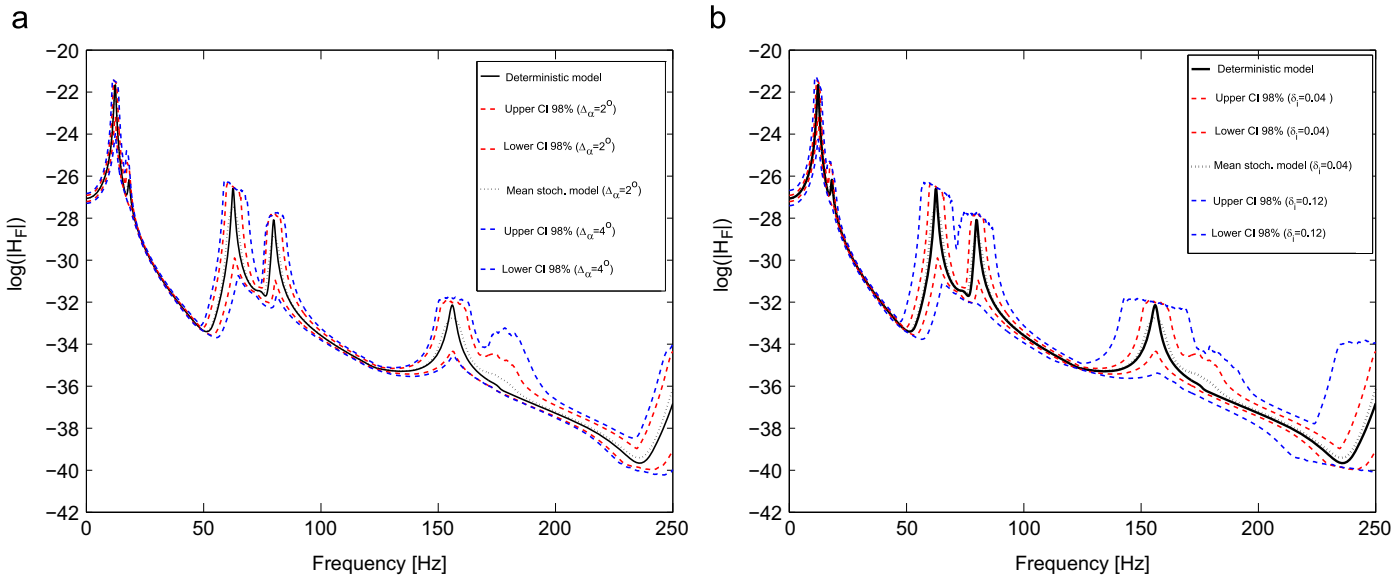

Fig. 6. FRFs simulated with the PPA for the lamination CAS(15). (a) with $\delta_i = 0.04$ and (b) with $\Delta_\alpha = 2^\circ$.

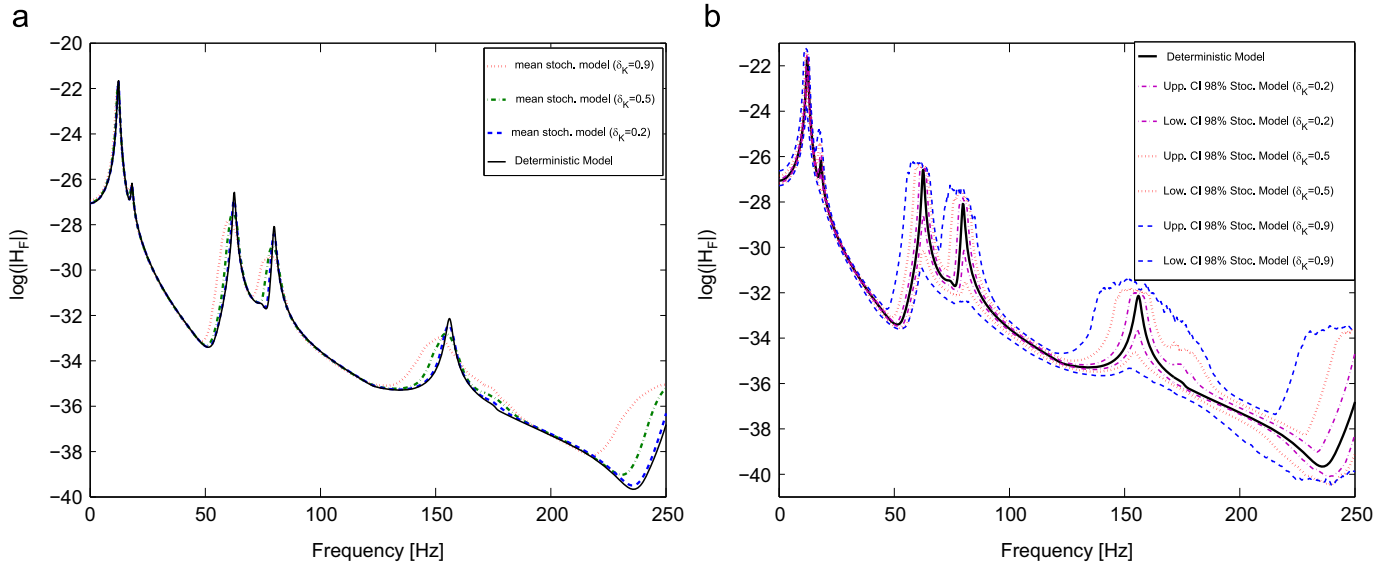

Fig. 7. FRFs simulated with the NPPA for the lamination CAS(15). (a) Mean responses. (b) Confidence intervals.

properties has been fixed in its lower value ($\delta_i = 0.04$, $i = 5, \ldots, 10$, and the angular dispersion of reinforcement is prescribed, in turns, in the minimum ($\Delta_\alpha = 2^\circ$) and maximum ($\Delta_\alpha = 4^\circ$) limits, whereas in the case of Fig. 6(b) the angular dispersion parameter is settled in $\Delta_\alpha = 2^\circ$ and the dispersion parameters of the elastic properties can have, in turns, the minimum ($\delta_i = 0.04$, $i = 5, \ldots, 10$) and maximum ($\delta_i = 0.12$, $i = 5, \ldots, 10$) values.

Fig. 7 exemplifies the FRFs calculated from the Monte Carlo simulations in which the NPPA was employed. Effectively in Fig. 7 (a) one can see the responses of the deterministic model and the mean responses for given values of the non-parametric dispersion parameter $\delta_{\mathbb{K}}$. On the other hand, in Fig. 7(b) one can see the deterministic response and the bounds of the 98% confidence intervals for the same values of $\delta_{\mathbb{K}}$. It can be observed that there are some intervals where the uncertainty of the model does not affect the sensitivity the dynamic response, for example in the frequency range of $[22, 48]$ Hz. On the other hand, in the proximities of the peaks there is a strong influence of the uncertainty in the model as well as it is observed in the studies carried out with the PPA.

Fig. 8(a) and (b) presents the histograms of the realizations performed at frequencies $f = 15.5$ Hz and $f = 25.0$ Hz, respectively. Fig. 8(a) corresponds to an excitation frequency between the first and second natural frequencies of the beam, whereas Fig. 8(b) corresponds to an excitation frequency between the second and third natural frequencies. It could be observed that the dispersion is larger as the excitation frequency is near to the peaks of the FRF which is in consonance with the behavior observed in Figs. 6 and 7 where there is evidence of no strong influence of uncertainty, in both properties or models, in the intervals of frequency $[22, 48]$ Hz and $[105, 120]$ Hz.

In the subsequent figures, an evaluation of the uncertainty propagation, for different types of laminates and boundary conditions, is shown. All these cases are simulated with the NPA, in which the uncertainty measure is settled in $\delta_{\mathbb{K}} = 0.6$. In Fig. 9 the FRFs for different boundary conditions of the case of lamination CUS(45) are shown. In both cases the deterministic response, the mean stochastic response and the 98% confidence interval are depicted. As it is possible to see, there are some intervals where the response is not that sensitive to the variability despite the higher value of the

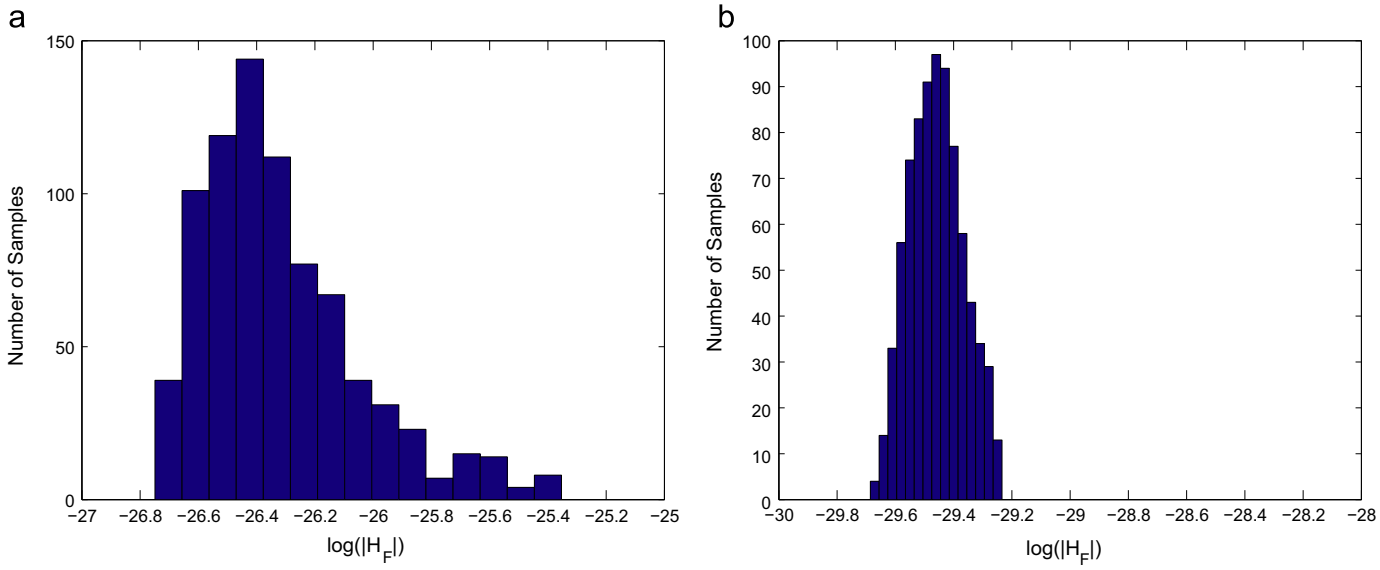

Fig. 8. Histograms at given frequencies of CAS(15). (a) $f = 15.5$ Hz. (b) $f = 25.0$ Hz.

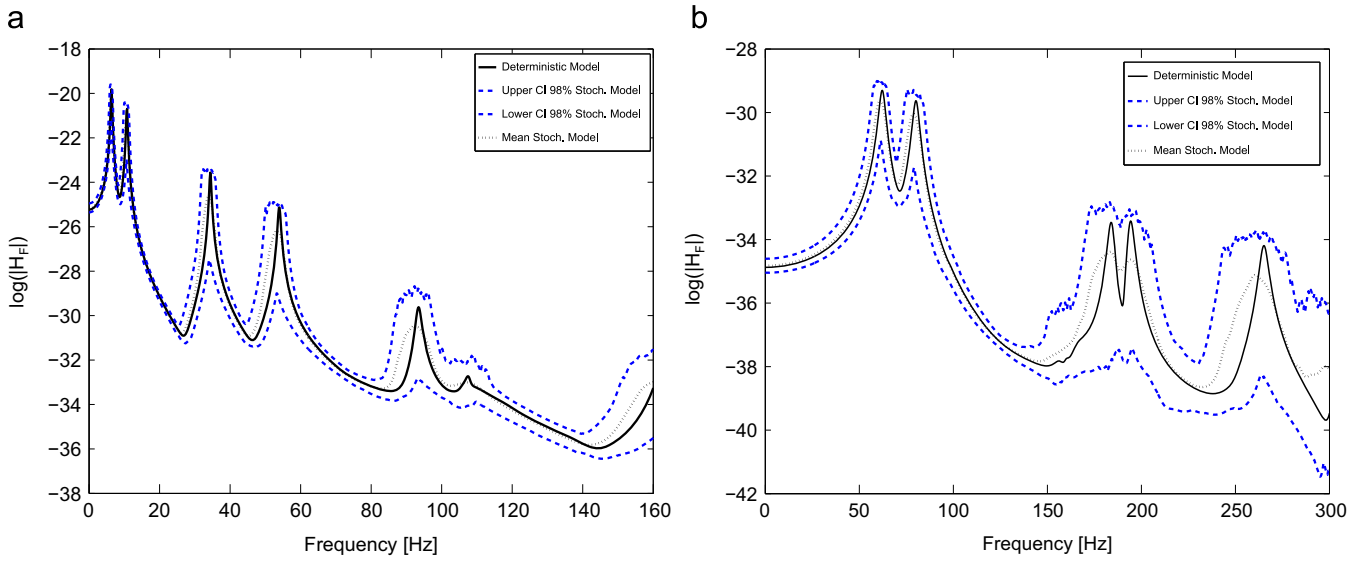

Fig. 9. FRFs for a CUS(45) lamination. (a) Clamped–free. (b) Clamped–clamped.

uncertainty assumed in the model. The same information is shown in Fig. 10 but for the case of lamination CAS(45).

A way to identify the frames where the FRFs manifest the lowest sensibility to the uncertainty of input (properties or modeling) is by means of the calculation of the coefficient of variation (*CV*) defined as the ratio of standard deviation to the mean. A suitable a limit to the *CV* can be imposed and then the frequency bands in which the FRFs have a limit of variability can be found. In Table 4 the frequency bands, where $CV \leq 0.1$, are presented for different cases of stacking sequences and boundary conditions.

It is possible to see in Table 4, for the case of the clamped–clamped boundary condition, that the band of frequencies in which the $CV \leq 0.1$ (or in other words: of lower sensitivity to uncertainties) is normally narrow or an empty set. Clearly if a higher *CV* is accepted, e.g. $CV \leq 0.2$, the frequency-bounds of lower sensibility to uncertainty will increase. Stacking sequences with full or partial reinforcement of $\alpha = 45^\circ$ are the exception, i.e. the laminates with the lower values of coefficients $\overline{A}_{11}/\overline{A}_{66}$ and $\overline{A}_{11}/\overline{D}_{66}$. On the other hand, for the case of clamped–free boundary condition, there is evidence of a band of frequencies that has low sensitivity to uncertainties for the stacking sequences evaluated.

5. Conclusions

In this paper a study about the quantification of uncertainty and its propagation in the dynamics of thin-walled composite-curved beams has been carried out. The parametric probabilistic approach (PPA) and the non-parametric probabilistic approach (NPPA) have been employed. The later approach allows the analysis of uncertainties in the conception of the model as a whole entity. The effect of shear deformation has been revisited and its influence in the context of an uncertain model has been evaluated. Both approaches have been compared and employed and despite the common procedural differences, the following remarks can be made:

- The propagation of uncertainty in the dynamic response of composite thin-walled curved beams is more sensitive to the

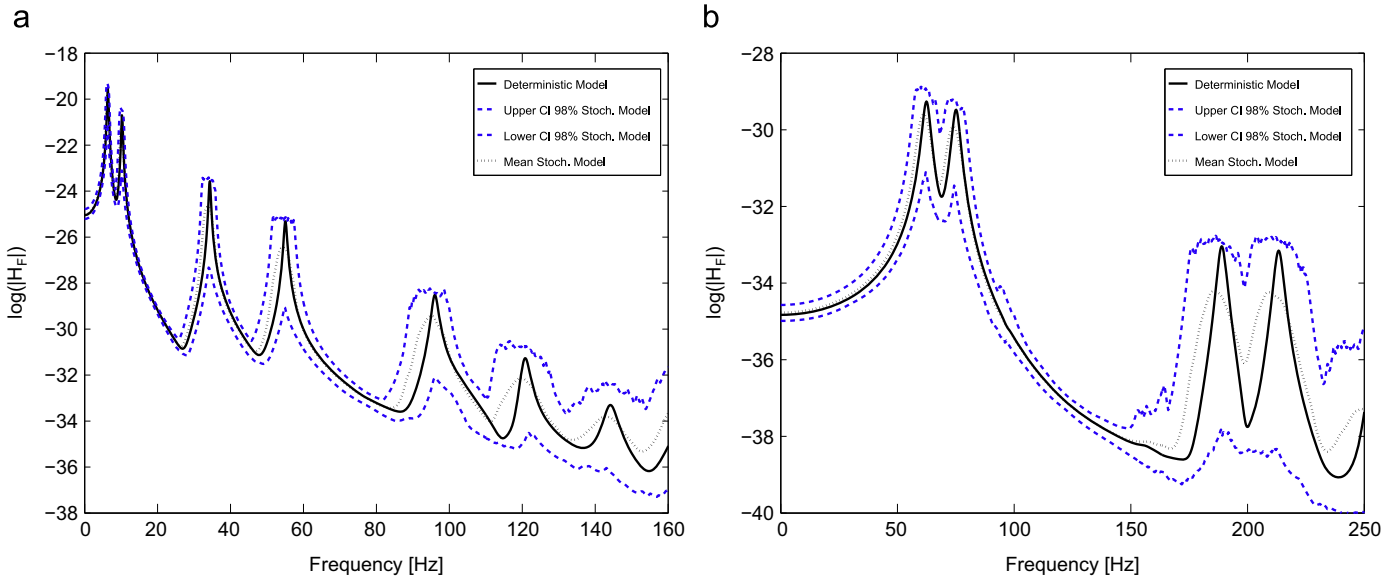

Fig. 10. FRFs for a CAS(45) lamination. (a) Clamped–free. (b) Clamped–clamped.

Table 4
Frequency-bands where $CV \leq 0.1$.

Laminate type	Clamped–free	Clamped–clamped
CUS(45)	[15.2, 26.5]	[0.0, 18.2]⋃[104.5, 133.2]
CAS(45)	[14.4, 25.8]	[0.0, 17.5]⋃[110.6, 137.8]
CUS(0|45)	[28.4, 54.9]⋃[107.1, 141.2]	[0.0, 15.3]
CAS(0|45)	[28.2, 57.6]⋃[109.5, 145.7]	[0.0, 18.5]
CUS(15)	[22.9, 47.3]⋃[79.7, 106.7]	∅
CAS(15)	[21.6, 49.8]⋃[104.1, 127.9]	∅
CUS(0|15)	[27.1, 55.9]⋃[94.5, 118.6]	∅
CAS(0|15)	[23.6, 57.5]⋃[101.2, 132.1]	∅
CUS(0|90)	[20.6, 47.1]⋃[79.1, 104.8]	∅
CUS(0|0)	[25.1, 51.1]⋃[85.7, 110.7]	∅

variability of the elastic properties that to the variability of angular reinforcement.

- The variability of the dynamic response is strongly influenced by the type of elastic coupling inherent to the lamination schemes.
- The non-parametric probabilistic approach can face uncertainties in the modeling theories for example the type of shear flexibility theory employed.
- From the viewpoint of the high variability observed in the FRFs of composite curved beams, the incorporation of γ_{xn} in the constitutive equations, as a sum of stiffness, does not offer an enhancement in the mechanics of composite curved beams.
- Although the conclusions of the previous item are known fact, the effects of thickness shear deformation (i.e. γ_{xn}) as a part of model uncertainty have been evaluated and, for some cases, quantified.
- There is evidence of the presence of regions that have a lower sensitivity to the uncertainty of the model and/or parameters. Although the width and the location of the frequency-bands are case dependent on the boundary conditions and dimensions of the beam.

Nevertheless, there are other concerns related to the uncertainty of the beam model and the parameters themselves that have not been analyzed, for example, the correlation among elastic properties as well as other random variables, other types of cross section, etc. In order to characterize the dynamics of composite beams with uncertainties, their influence should be quantified. However these studies are addressed for further extensions to the present investigations.

Acknowledgments

The authors recognize the support of Universidad Tecnológica Nacional (Project no. AMUTI0002194TC) and CONICET of Argentina and FAPERJ and CNPq of Brazil.

Appendix A. Definition in-extenso of matrices and vectors employed in the principle of virtual works

The vector of external forces $\tilde{\mathbf{P}}_X$ and the matrix of mass coefficients $\mathbf{M}_m$ can be calculated in the following form:

$$\tilde{\mathbf{P}}_X = \int_A [\overline{X}_x \ \overline{X}_y \ \overline{X}_z]\mathbf{G}_m \frac{R\,dy\,dz}{R+y}, \tag{A.1}$$

$$\mathbf{M}_m = \int_A \rho(y,z)\mathbf{G}_m^T\mathbf{G}_m \frac{R\,dy\,dz}{R+y}, \tag{A.2}$$

where $\overline{X}_x$, $\overline{X}_y$ and $\overline{X}_z$ are general volume forces, whereas

$$\mathbf{G}_m = \begin{bmatrix} 1+y/R & 0 & -y & 0 & z-\omega/R & 0 & -\omega \\ 0 & 1 & 0 & 0 & 0 & -z & 0 \\ 0 & 0 & 0 & 1 & 0 & y & 0 \end{bmatrix}, \tag{A.3}$$

The vector of natural boundary conditions $\tilde{\mathbf{B}}_X$ can be written in the following subsequent form:

$$\tilde{\mathbf{B}}_X = \begin{Bmatrix} -\overline{Q}_x+\overline{M}_z/R+Q_x-M_z/R \\ -\overline{Q}_y+Q_y \\ -\overline{M}_z+M_z \\ -\overline{Q}_z+Q_z \\ -\overline{M}_y+\overline{B}/R+M_y-B/R \\ -\overline{T}_{sv}-\overline{T}_w+T_{sv}+T_w \\ -\overline{B}+B \end{Bmatrix}, \tag{A.4}$$

where $\overline{Q}_x$, $\overline{Q}_y$, $\overline{Q}_z$, $\overline{M}_y$, $\overline{M}_z$, $\overline{T}_w$ and $\overline{T}_{sv}$ are prescribed forces and moments applied at the boundaries.

References

[1] Barbero E. Introduction to composite material design. New York, USA: Taylor and Francis Inc.; 1999.
[2] Jones R. Mechanics of composite material. New York, USA: Taylor and Francis Inc.; 1999.
[3] Bauld N, Tzeng L. A vlasov theory for fiber-reinforced beams with thin-walled open cross sections. Int J Solids Struct 1984;20(3):277–97.
[4] Bauchau O. A beam theory for anisotropic materials. J Appl Mech 1985; 52(2):416–22.
[5] Wu X, Sun C. Vibration analysis of laminated composite thin walled beams using finite elements. AIAA J 1990;29(5):736–42.
[6] Librescu L, Song O. On the aeroelastic tailoring of composite aircraft swept wings modeled as thin walled beam structures. Compos Eng 1992;2(5):497–512.
[7] Song O, Librescu L. Free vibration of anisotropic composite thin-walled beams of closed cross-section contour. J Sound Vib 1993;167(1):129–47.
[8] Kim C, White S. Thick walled composite beam theory including 3d elastic effects and torsional warping. Int J Solids Struct 1997;34(31):4237–59.
[9] Cesnik C, Sutyrin V, Hodges D. Refined theory of composite beams: the role of short-wavelength extrapolation. Int J Solids Struct 1996;33(10):1387–408.
[10] Cortínez V, Piovan M. Vibration and buckling of composite thin-walled beams with shear deformability. J Sound Vib 2002;258(4):701–23.
[11] Piovan M, Cortínez V. Mechanics of shear deformable thin-walled beams made of composite materials. Thin-Walled Struct 2007;45:37–62.
[12] Piovan M, Cortínez V. Mechanics of thin-walled curved beams made of composite materials, allowing for shear deformability. Thin Walled Struct 2007;45:759–89.
[13] Sriramula S, Chryssantopoulos M. Quantification of uncertainty modelling in stochastic analysis of frp composites. Composites: Part A 2009;40:1673–84.
[14] Sampson W. Modelling stochastic fibrous materials with mathematica. Springer-Verlag London Limited; 2009.
[15] Vickenroy G, Wilde W. The use of the Monte Carlo techniques in statistical finite element methods for the determination of the structural behavior of composite material structural components. Compos Struct 1995;32(1):247–53.
[16] Salim S, Yadav D, Iyengar N. Analysis of composite plates with random material characteristics. Mech Res Commun 1993;20(3):405–14.
[17] Pawar P. On the behavior of thin walled composite beams with stochastic properties under matrix cracking damage. Thin-Walled Struct 2011;49:1123–31.
[18] Mehrez L, Moens D, Vandepitte D. Stochastic identification of composite material properties from limited experimental databases. Part i: experimental database construction. Mech Syst Signal Process 2012;27:471–83.
[19] Mehrez L, Doostan A, Moens D, Vandepitte D. Stochastic identification of composite material properties from limited experimental databases. Part ii: uncertainty modelling. Mech Syst Signal Process: Uncertaint Model 2012;27:484–98.
[20] Soize C. Random matrix theory and non-parametric model of random uncertainties in vibration analysis. J Sound Vib 2003;263:893–916.
[21] Sampaio R, Cataldo E. Comparing two strategies to model uncertainties in structural dynamics. Shock Vib 2011;17(2):171–86.
[22] Ritto T, Sampaio R, Cataldo E. Timoshenko beam with uncertainty on the boundary conditions. J Brazil Soc Mech Sci Eng 2008;30(4):295–303.
[23] Piovan M, Ramirez J, Sampaio R. Dynamics of thin-walled composite beams: analysis of parametric uncertainties. Compos Struct 2013;105:14–28.
[24] Jaynes E. Information theory and statistical mechanics. Phys Rev 1957;106 (4):1620–30.
[25] Jaynes E. Information theory and statistical mechanics ii. Phys Rev 1957;108:171–90.
[26] Shannon C. A mathematical theory of communication. Bell Syst Tech 1948;27:379–423.
[27] M. Piovan, Estudio Teórico y Computacional sobre la mecánica de vigas curvas de materiales compuestos con secciones de paredes delgadas considerando efectos no convencionales [Ph.D. thesis]. Departamento de Ingeniería, Universidad Nacional del Sur; 2003.
[28] Bathe K-J. Finite element procedures in engineering analysis. Englewood Cliffs, NJ, USA: Prentice-Hall; 1996.
[29] Meirovitch L. Principles and techniques of vibrations. Upper Saddle River, NJ: Prentice-Hall; 1997.
[30] Yang W, Cao W, Chung T-S, Morris J. Applied numerical methods using matlab. New Jersey, USA: Wiley and Sons Inc.; 2005.
[31] Soize C. Maximum entropy approach for modeling random uncertainties in transient elasto-dynamics. J Acoust Soc Am 2001;109(5):1979–96.
[32] Soize C. A comprehensive overview of a non-parametric probabilistic approach of model uncertainties for predictive models in structural dynamics. J Sound Vib 2005;288(3):623–52.
[33] Rehfield L, Atilgan A, Hodges D. Non-classical behavior of thin-walled composite beams with closed cross sections. J Am Helicopter Soc 1990;35(3):42–50.
[34] Piovan M, Cortínez V. Transverse shear deformability in the dynamics of thin-walled composite beams: consistency of different approaches. J Sound Vib 2005;285(3):721–33.
[35] Minghini F, Tullini N, Laudiero F. Vibration analysis with second-order effects of pultruded frp frames using locking-free elements. Thin-Walled Struct 2009;47(2):136–50.
[36] Hodges D. Nonlinear composite beam theory. Reston, VA, USA: American Institute of Aeronautics and Astronautics Inc.; 2006.